

ENGINEERING RESEARCH INSTITUTE
THE UNIVERSITY OF MICHIGAN
ANN ARBOR

RESISTANCE TO UNSTEADY FLOW

I. Analysis of Tests with Flat Plate

John S. McNown
Louis W. Wolf

Project 2446

SANDIA CORPORATION
ALBUQUERQUE, N. M.

June 1956

TABLE OF CONTENTS

	Page
LIST OF FIGURES	iii
SUMMARY	iv
OBJECTIVE	iv
INTRODUCTION	1
THEORY	1
Inertial Effects	2
Resistance in Unsteady Flow	4
Characteristics of Standing Waves	5
EXPERIMENTATION	7
ANALYSIS OF RESULTS	9
Interpretation of $F(t)$	9
Analysis of Wave	11
CONCLUSION	13
APPENDIX	14
REFERENCES	15

LIST OF FIGURES

No.		Page
1.	Flow patterns.	3
2.	Relationship between C_D and k .	3
3.	Comparison of wave forms.	6
4.	Experimental equipment.	7
5.	Force-measuring system.	8
6.	Typical force and displacement record.	9
7.	Comparison of predicted and measured forces.	11
8.	Analysis of force variation.	12
9.	Effect of $k(t)$ on force prediction.	14

SUMMARY

Unsteadiness of flow affects the resistance of a blunt body because of the inertia of the fluid and because the pattern of flow in the wake is altered. Both the drag coefficient and the virtual mass for the body are variable with time. Provisional evaluations of these changes have been obtained from a study of the time variation of the force exerted on a plate placed normal to the primary flow resulting from a standing wave in a small tank. Because the phases of the inertial (acceleration-dependent) force and the drag (velocity-dependent) force differ by a quarter-period in the resulting motion, the wave system is preferable to unidirectional motions for preliminary studies.

Significant increases were found in both parts of the resistance. The virtual mass is high for blunt bodies because of the inevitable separation; the drag is greater because the separation pocket is usually incompletely formed. A theoretical correlation between the two kinds of resistance was formulated on the basis of a free-streamline flow past two plates as proposed by Riabouchinsky. For a properly assumed variation of the virtual mass, the observed results were predicted with acceptable accuracy.

OBJECTIVE

To measure the effects of unsteadiness of flow on the total resistance of submerged bodies and to interpret their effects so as to provide a basis for predicting resistance in large scale flows.

INTRODUCTION

Forces exerted on structures by the unsteady flow of a fluid are caused by combinations of effects due to the velocity, the acceleration, and the pressure gradient of the ambient flow. For bluff bodies, a wake is formed. Temporal changes in the shape of the wake, which forms if the structure is not streamlined, affect both the drag and the virtual mass. These combined effects occur if structures are subjected to large-scale blasts in air or to storm waves in water.

Estimates of the magnitudes of accelerative forces exerted by blasts on test blocks in the course of studies conducted by the Sandia Corporation indicated the importance of acceleration. The velocity can diminish so rapidly after the initial shock that the total force on a structure becomes zero or even negative well before the direction of flow changes. So little information on this and on other aspects of the resistance to unsteady flow was available that a research program was proposed. An oscillatory wave motion was selected for the first tests so that the effects of acceleration and velocity could be more easily separated. In addition, tests of unidirectional accelerated motion are planned.

The research program, which is sponsored by the Sandia Corporation, was undertaken in the laboratory of the Engineering Mechanics Department at The University of Michigan. A tank had already been constructed for the purpose, and preliminary tests had proven the feasibility of the undertaking. Limited support for the preliminary tests had been provided by the Engineering Research Institute of the University. The present one-year contract was initiated October 15, 1955, between the University and the corporation. The project is supervised by John S. McNown. Most of the experiments and analyses have been conducted by L. W. Wolf with the assistance of K. Aoki.

THEORY

In classical theory only background material is available for the analysis of resistance in unsteady flow. The concept of virtual mass is well

understood as it applies to accelerated relative motion of fluids and submerged bodies.¹ Also, considerable progress has been made in the development of the theory of wave motion.²

INERTIAL EFFECTS

If a body is accelerated in a fluid, the various elements of the fluid are also accelerated. The integrated effect of these is a force and a reaction between the body and the fluid. Thus,

$$\rho \iiint \frac{dv}{dt} dx dy dz = kM' \frac{dV}{dt} ,$$

in which the integral is taken throughout the fluid. The virtual mass kM' is defined in terms of a coefficient k multiplied by a reference mass M' which is usually the mass of fluid displaced by the body. For thin, flat plates or for disks the displaced mass is zero. Hence, a circular cylinder or a sphere of the same section is used as a basis of reference. Virtual mass can also be introduced from a consideration of kinetic energy. If the velocity of a submerged body is increased, so is the kinetic energy of the fluid around it. Consequently, work is done and a force is exerted on the fluid. For flows describable in terms of velocity potentials, the kinetic energy of the flow and its time derivative are used in determining k .

Virtual-mass coefficients are available for only a few mathematically simple bodies. For all elliptic cylinders with one axis parallel to the direction of flow, the virtual mass is equal to the mass displaced by a circular cylinder for which the diameter is the transverse axis of the ellipse.¹ The flat plate in Fig. 1a is a limiting case. An expression in elliptic functions was developed by Riabouchinsky for cylinders with rectangular cross sections.³ Also available in terms of elliptic integrals are coefficients for any ellipsoid, provided only that one axis is parallel to the direction of motion.¹ For all of these cases, irrotational flow without separation is assumed.

Because separation occurs in flow past any body which is not well streamlined, the theoretical results are not necessarily useful in analyzing flows past structures of conventional design. A more realistic representation of flow past a flat plate was proposed by Riabouchinsky,³ in which a second plate downstream of the first closes the flow as shown in the left part of Fig. 1b. The cavity, bounded by the two plates and the connecting free streamlines, is a mathematical approximation to actual wakes also shown schematically. Birkhoff et al.⁴ extended this analysis and presented drag coefficients for various cases. The method was again extended recently to include the evaluation of the virtual-mass coefficient for systems with various spacings of the plates.⁵ The results are shown in Fig. 2. Other ways of achieving finite cavities are the reentrant jet of Gilbarg⁶ and the parallel afterbody of Roshko.⁷

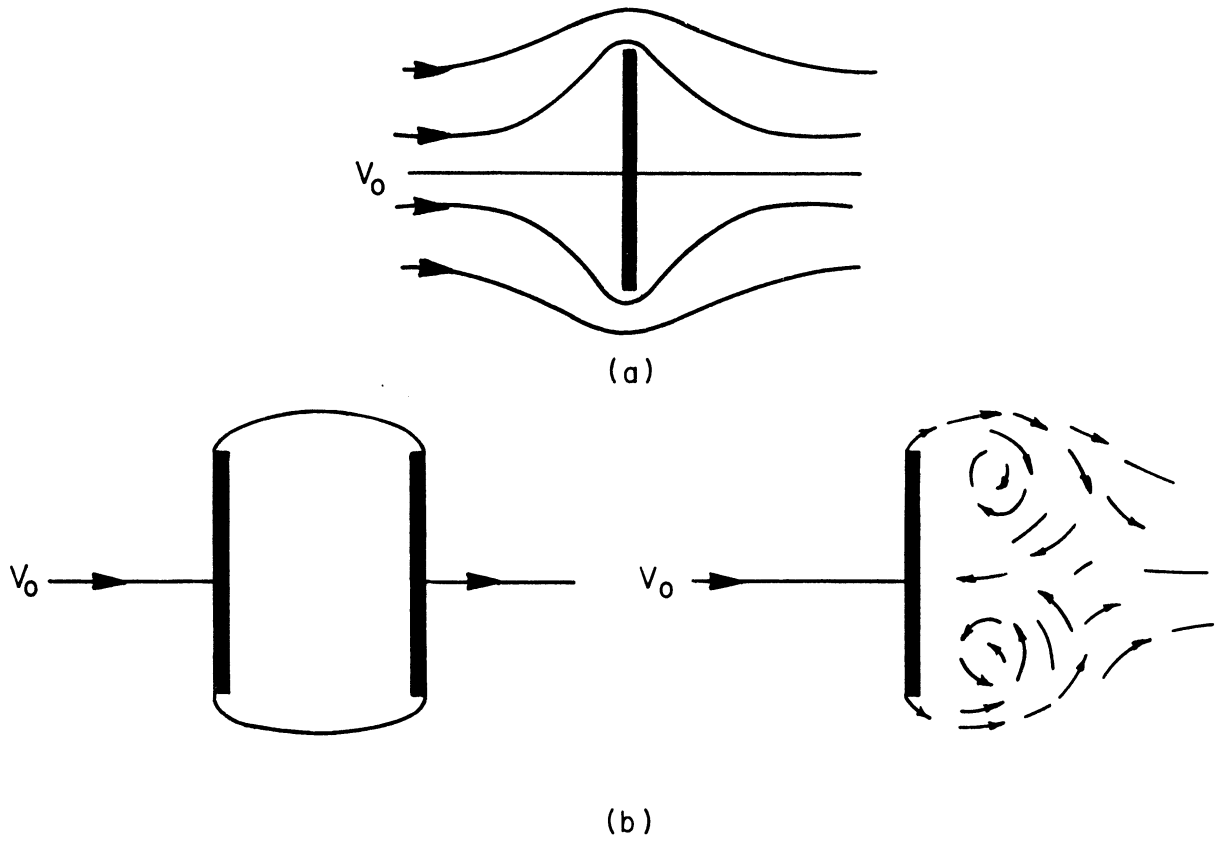


Fig. 1. Flow patterns.

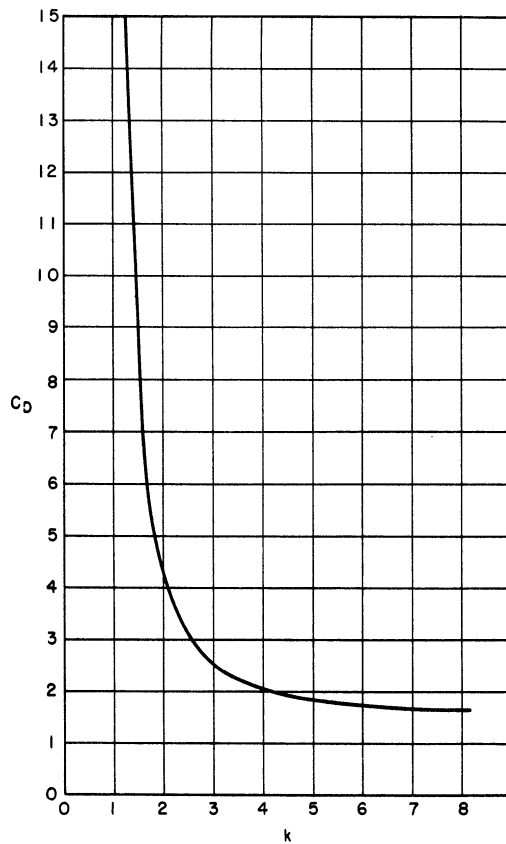


Fig. 2. Relationship between C_D and k .

The classical theory without separation is appropriate for motions in which the displacement is small. It has been used for determining the forces on dams during earthquakes,^{8,9} for studies of bodies vibrating in liquids,^{10,11} and for computations of gust and vibration loadings of airplane wings. Considerable discrepancy is found between the results of studies of this type and those obtained for flows in which the amplitude of the motion is large enough for a separation pocket to occur. This had led to some disagreement in the definition of k , as indicated by the published discussion¹² of the paper by Stelson and Mavis.

RESISTANCE IN UNSTEADY FLOW

Analysis of the action of accelerated flow past a flat plate is seriously complicated by several consequences of the unsteadiness of flow. Even the drag coefficient, which is usually considered to be dependent on the velocity alone, can be altered because the wake can be larger or smaller than that occurring for steady flow at a given velocity. Also, a longitudinal pressure gradient exists if the velocity is changing even in the absence of a body. Finally, the virtual-mass coefficient is in turn dependent on the shape of the pocket, as shown in Fig. 1, and both its magnitude and its time derivative affect the force. These various contributions to the resistance can be represented quantitatively by the formula

$$F = \int_S p_x dS + C_D A \frac{\rho V^2}{2} + M' \frac{d(kV)}{dt}, \quad (1)$$

in which p_x is the x-component of the ambient pressure in the absence of the body, S an element of the surface area, C_D the coefficient of drag, A the cross-sectional area of the body, and V the ambient velocity. If the body is accelerated through an otherwise quiet fluid, the pressure gradient becomes zero and the force required to accelerate the body must be added.

Difficult though an analysis based on Equation 1 may be, the separation of the various parts is less difficult for an oscillatory motion than it is for unidirectional accelerated motion. For the former, the acceleration and velocity are out of phase by a quarter period, and each is zero at the time the other is a maximum. Hence, some possibility of distinguishing the two effects exists. In fact, this concept has been used by Reid and Bretschneider¹³ to evaluate k and C_D . Each was assumed to have at all times the constant value indicated at the moments for which the other force was zero. However, as already explained, these effects are dependent on the time history of the motion. No simple system based on constant values for either C_D or k can be complete. In laboratory studies of bodies which are accelerated and moving continuously in one direction, the effects of velocity and acceleration are not easily separable. In such a study of an accelerated disk, Iverson¹⁴ proposed an overall coefficient in which the two effects are combined. To

obtain an understanding which will apply to a variety of flows, these effects must be separated.

CHARACTERISTICS OF STANDING WAVES

The characteristics of the standing wave used in the present study have a direct bearing on the results obtained. The classical theory of irrotational wave motion of very small amplitude is well established.¹ A velocity potential can be written and all essential characteristics of the flow are defined. A sine wave is obtained for the free surface,

$$\eta = a \cos \frac{\pi x}{L} \cos \frac{2\pi t}{T}, \quad (2)$$

in which η represents the displacement of the free surface from the equilibrium position, a the amplitude of the wave, L the length of the tank ($L = \lambda/2$), and T the period of the motion. The velocity at the nodal plane is given by the expression

$$u = \frac{aTg}{2L} \frac{\cosh [k(z + H)]}{\cosh (kH)} \sin \frac{\pi x}{L} \sin \frac{2\pi t}{T}, \quad (3)$$

in which z is the vertical coordinate taken as positive upward and H is the depth of water. The period of the motion is dependent only on the acceleration of gravity and the dimensions of the system:

$$\left(\frac{2\pi}{T}\right)^2 = \frac{\pi g}{L} \tanh \frac{\pi H}{L}. \quad (4)$$

As the relative amplitude of the wave (a/λ) increases, the foregoing theory becomes less exact. Furthermore, no single method of improving the analysis serves for the entire range of relative depths (H/λ). For waves in moderately shallow water, as in these experiments, the wave form is called cnoidal because the free surface is described in terms of the cn elliptic function:

$$\eta = -a_2 + (a_1 + a_2) \left[\text{cn}^2(\alpha - \beta, m) + \text{cn}^2(\alpha - \beta, m) \right], \quad (5)$$

in which

$$\alpha = \frac{2F(m)}{\lambda}, \quad \beta = \frac{2F(m)}{\lambda} ct,$$

$$m = \sqrt{\frac{a_1 + a_2}{a_1 + a_3}}, \quad c = \frac{\lambda}{T} = \sqrt{gH} \left[\left(1 + \frac{a_1}{H}\right) \left(1 - \frac{a_2}{H}\right) \left(1 - \frac{a_3}{H}\right) \right]^{\frac{1}{2}}.$$

The quantities a_1 and a_2 represent distances from the undisturbed water level

to the crests and troughs, respectively, and c represents the wave celerity. The wave length and depth are related:

$$\frac{\lambda}{H} = 2\sqrt{\frac{4H}{3(a_1 + a_3)}} F(m) .$$

Finally, a_3 is defined implicitly by

$$a_1 + a_3 E(m) = a_3 F(m) .$$

F and E are complete elliptic integrals of the first and second kinds. The details of this theory are presented by Keulegan and Patterson.¹⁵ Significant differences between a sinusoidal and a cnoidal wave are apparent in Fig. 3 in that (1) the crests of the latter are higher and narrower than the troughs, whereas the sine wave is symmetrical, and (2) no true node exists for the cnoidal pattern.

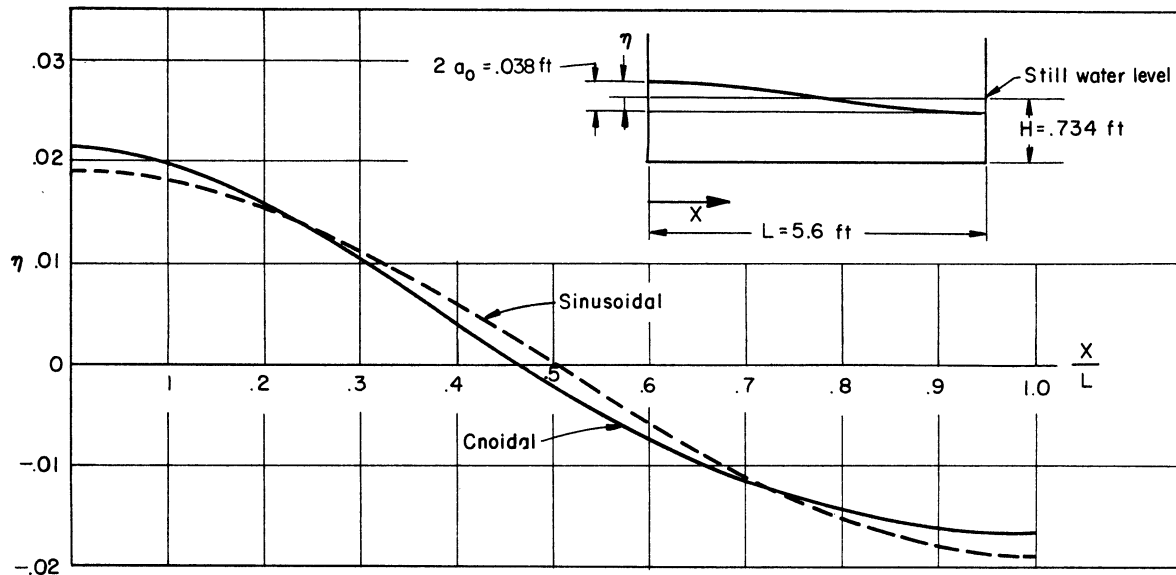


Fig. 3. Comparison of wave forms.

Consideration of these various theoretical results is essential if one is to bring to bear all available information on this complex problem. The virtual mass of the body is the very heart of the problem. The wave is the imposed motion and its characteristics must be known in detail. The accuracy of measurements of the wave can be assessed if the profile can be defined analytically. Although many features of the occurrence are not yet understood, the available theories provide a strong framework for the interpretation of the results.

EXPERIMENTATION

All measurements have been made for motions resulting from a standing wave in a small rectangular tank. The tank is 5.6 ft long, 2 ft wide, and will hold depths of water up to 1.2 ft (Fig. 4). The tank is made of stainless steel with Lucite side walls. A standing wave is created by means of a constant-speed motor acting through a speed reducer and an eccentric to give a nearly simple harmonic motion in the vertical direction to a wooden plunger at the surface of the water near one end of the tank.

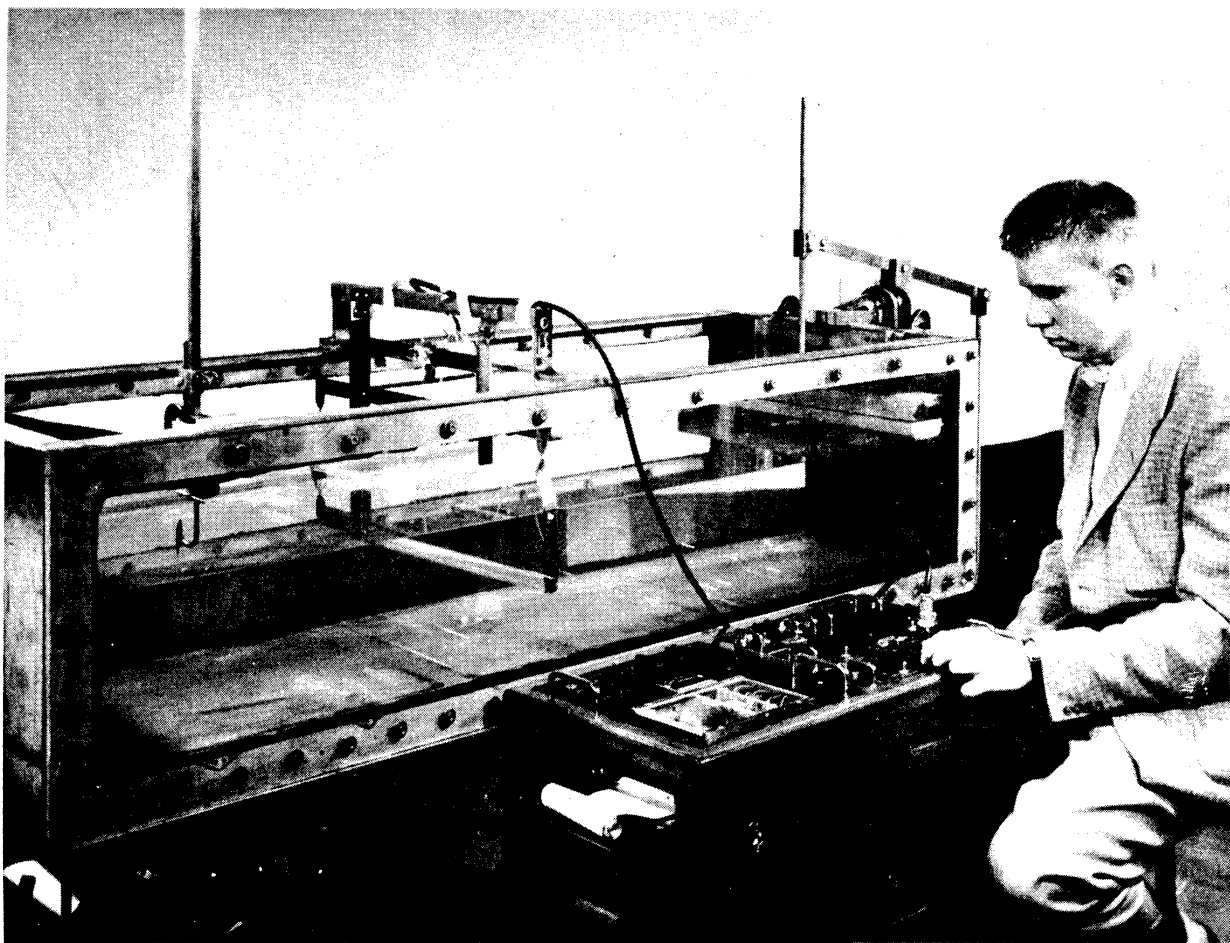


Fig. 4. Experimental equipment.

The period of the drive mechanism is 2.37 sec. The depth of the water is adjusted so that the fundamental mode of the tank from Equation 4, is the same as that of the drive. As the amplitude of the wave is increased, it is necessary to increase the water depth slightly to keep the period of the wave equal to that of the drive.

A brass plate 1 in. x 24 in. was suspended from roller bearings at mid-length and at mid-depth of the tank. Later the suspension was changed

from roller bearings to a set of elastic hinges to eliminate any possibility of friction interfering with the measurements (Fig. 5). The system was restrained from significant displacement by a Statham strain bridge (Model GI-48-675), and the signal thus created was fed into one channel of a Sanborn recorder (Model 60-1300) giving a measure of the variation with time of the force exerted on the plate by the water. A typical record is shown in the lower half of Fig. 6. The system was statically calibrated by hanging known weights on the arm extending from the suspension.

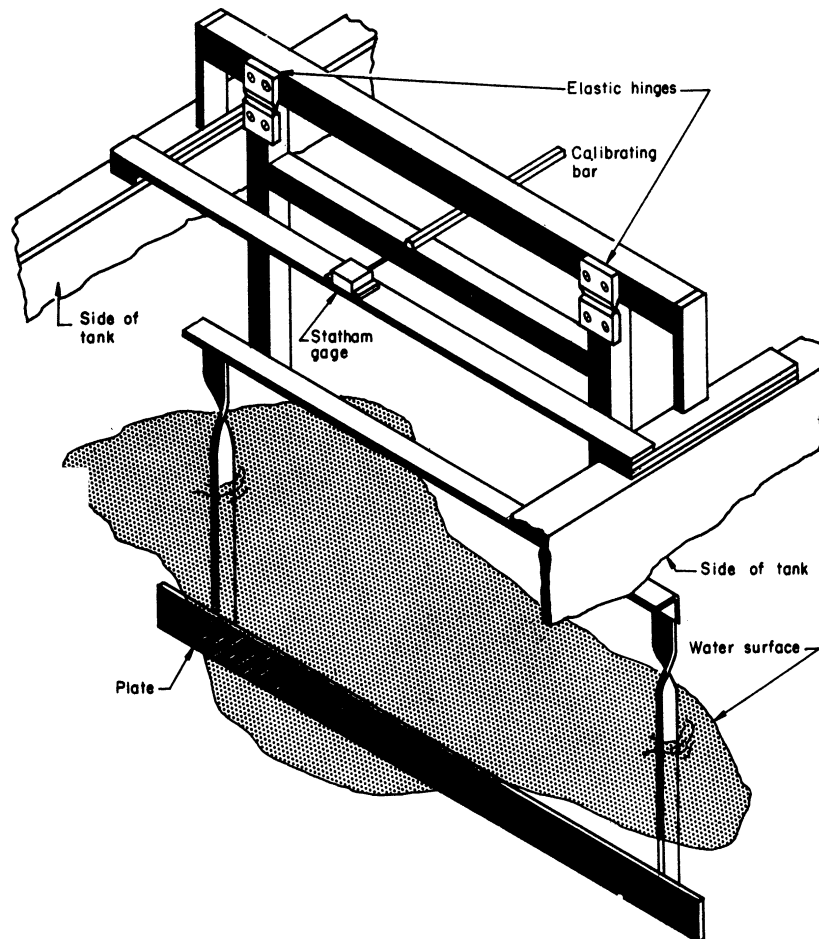


Fig. 5. Force-measuring system.

To measure the state of the water motion, a depth gage consisting of partially immersed resistance wires, designed to give linear readings with depth, was placed at the end of the tank away from the plunger. The signal from it was calibrated and supplied to the second channel of the Sanborn recorder. A continuous record of the amplitude and wave form was thus obtained. A typical record of the wave profile is shown in the upper portion of Fig. 6. The amplitude of the wave was checked independently by means of a point-and-hook gage near the end of the tank. Reliable readings to the nearest 0.001 in. were obtained. The height (double amplitude) of the wave was varied from 0.030 ft to 0.070 ft.

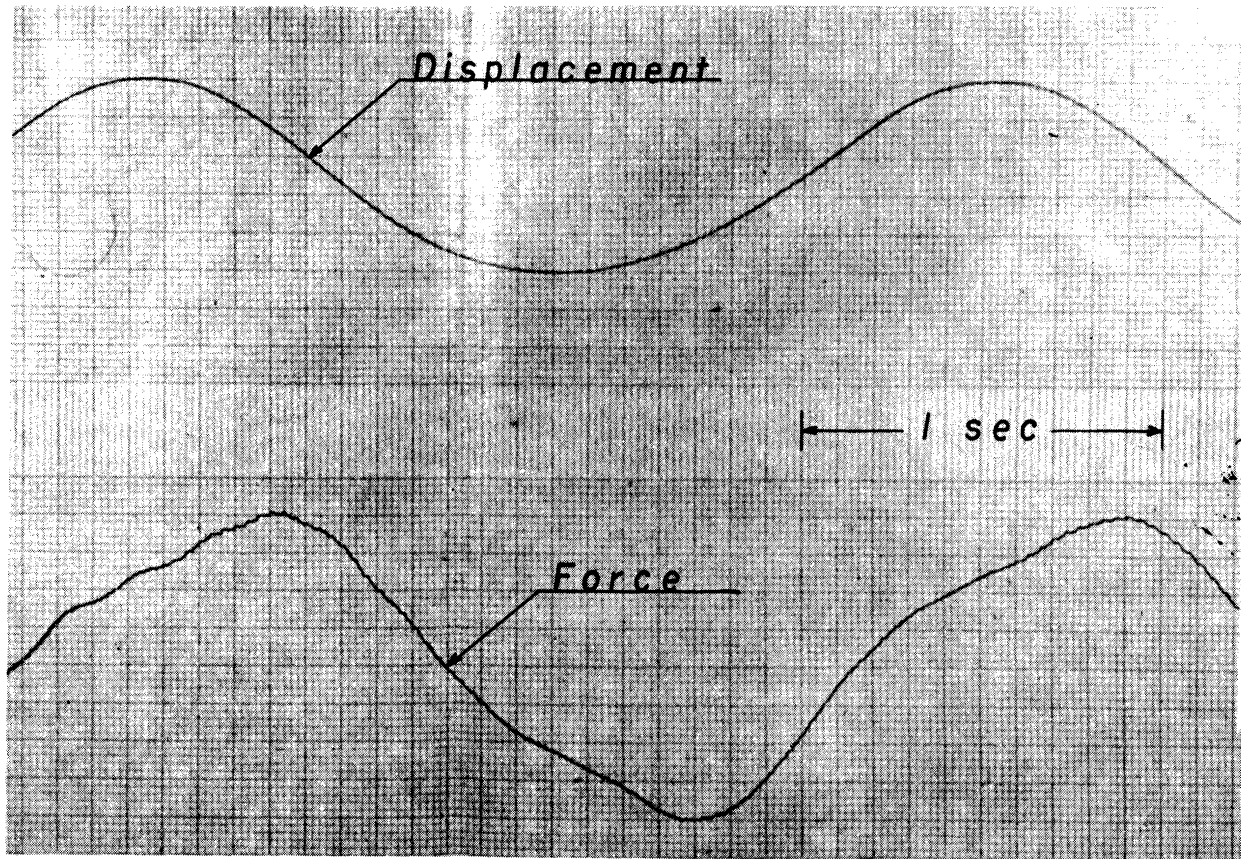


Fig. 6. Typical force and displacement record.

ANALYSIS OF RESULTS

INTERPRETATION OF $F(t)$

Several methods of predicting the force on the plate were tested by comparisons with the observed force. The entire cycle was considered rather than maxima or approximate constant values for the coefficients of drag and of virtual mass. The approaches used ranged from the empirical to the theoretical. For the latter, calculations were based on the theoretical results for the finite wake of Riabouchinsky (Fig. 2).

Perhaps the simplest of comparisons is one in which (1) the drag coefficient is assumed to be constant and to have the same value as is obtained for steady flow (approximately 2.0), and (2) the virtual-mass coefficient is assumed to be unity as it would be for irrotational flow without separation. Forces predicted in this way are considerably too small and improperly phased. The need for larger values of C_D and k , already discussed, was thus qualitatively substantiated by the experiments. Also, no arbitrary choice of larger

but constant values for these coefficients could be made for which predictions were compatible with the data.

An entirely theoretical method was attempted—also without success. The coefficients were assumed to be related as shown in Fig. 2. Also, the variations of the values were assumed to be controlled so that a minimum force was produced at any time. Out of the infinite number of possible variations of k (or C_D) with time, it was postulated that the one requiring the least work would be the most likely. No firm physical basis for this idea exists, nor did it prove to be a workable hypothesis. Despite many and varied attempts, no complete prediction could be formulated.

Graphical methods progressed fairly well for a part of a cycle, but a point was invariably reached for which the guiding hypothesis became ineffective. Approximate mathematical formulations were no more successful. The degree of freedom implicit in Equation 1 is such that a theoretical value of zero is possible for all times unless k is restricted. Although k is known to be restricted to positive values (probably greater than unity), this condition could not be easily imposed. Consequently, this method of approach was dropped.

Good predictions were finally achieved by combining the relationship of Fig. 2 with an arbitrarily assumed variation of k with time. Various trends for $k(t)$ were tested against the data by means of a stepwise integration of Equation 1 described in the Appendix. The achievement of a realistic result imposed a severe restriction on the assumed $k(t)$; a quantitative correspondence with the data was an even more stringent restriction. The results obtained for various assumed values of $k(t)$ are illustrated in the Appendix.

Once acceptable results were obtained for a wave height of 0.040 ft, the same $k(t)$ was used for all four amplitudes for which measurements of $F(t)$ had been made. The computed and observed forces are compared in Fig. 7. Closer correspondence could have been obtained in several ways. However, further efforts in this direction do not seem worthwhile at present because of the several approximations involved in various parts of the process. The extent to which the predictions and observations correlate justifies in a general and qualitative way the method of approach.

The two primary contributions to the total force are separated in Fig. 8. Also shown are the variations of velocity and acceleration and the assumed $k(t)$. The extent to which the curves for the acceleration and the acceleration-dependent force are disproportionate or out of phase is a measure of the importance of the time derivative of k . That is, the last term in Equation 1 can be separated into two parts:

$$\frac{d(kV)}{dt} = V \frac{dk}{dt} + k \frac{dV}{dt} .$$

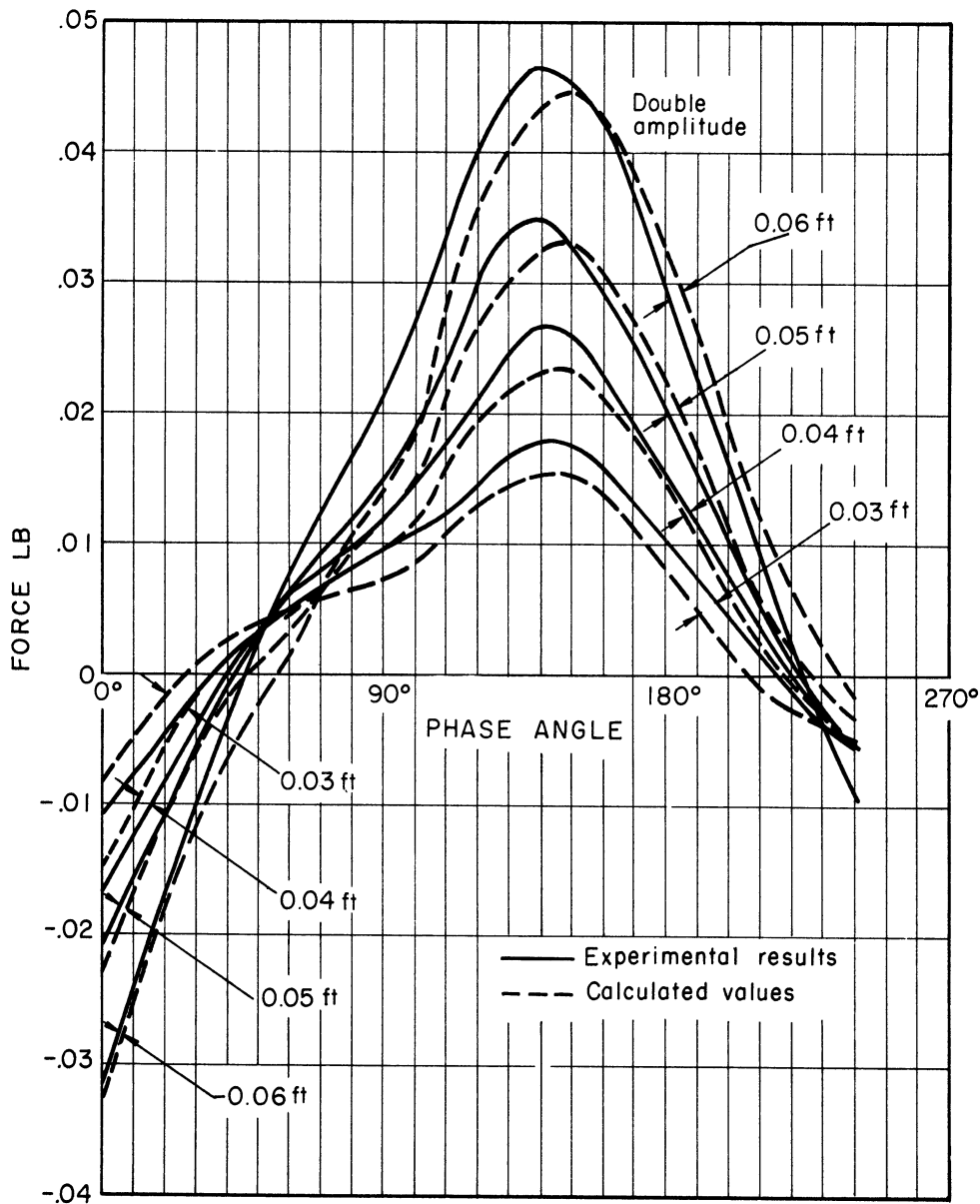


Fig. 7. Comparison of predicted and measured forces.

If k were truly a constant coefficient, the first part would be zero. Instead, its contribution is significant.

ANALYSIS OF WAVE

Among the limitations on the present study is a minor uncertainty as to the exact motion created by the wave. The dependence of the period of the wave on the amplitude is not defined explicitly by theory. Nor is the precise motion in the vicinity of the plate known. A cnoidal wave form was observed except for the portion of the tank near the plunger. However, sinusoidal variations were assumed for both velocity and acceleration. The discrepancies are not likely to be significant.

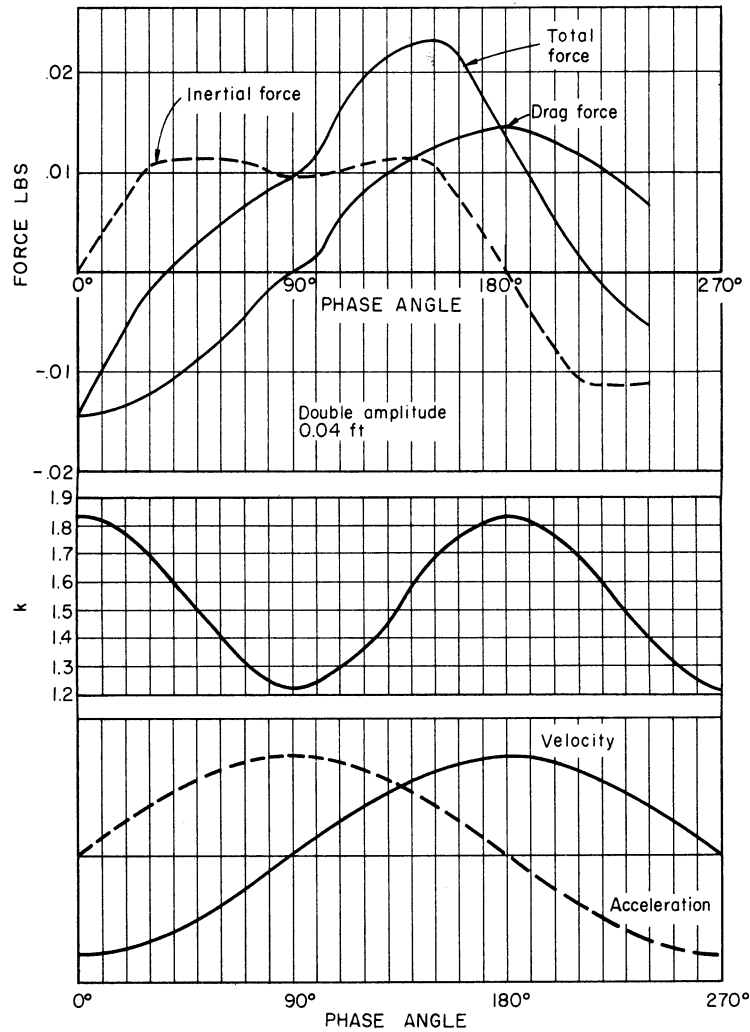


Fig. 8. Analysis of force variation.

Various secondary factors may alter the data somewhat. The maximum value for the Reynolds number was 1750. The upper limit of the variations due to viscosity is approximately 10^3 , so that a part of the data may have been affected by viscosity. There may also have been small irregularities at the ends of the plate or at the supports. The force on a one-inch plate in water only 9 inches deep may be affected by the bottom of the tank or the free surface. Finally, the water velocity decreases in accordance with Equation 3 from a maximum at the top to about 90% of this value at the bottom. An average value was used.

The proposed theory can be criticized because the assumed pattern for the variable wake is much simpler than that observed. Certainly, the relationship between k and C_D presented in Fig. 2 should be considered as representative rather than exact. A cavity bounded by two plates connected by free streamlines is not a good approximation for the early stages of wake formation. Instead, cylindrical vortices form and grow into a wake. Once formed, of

course, these vortices may persist. It is probably for this reason that the value of k was always greater than unity. A theoretical formulation based on a growing vortex may be possible.

Although none of the foregoing discrepancies is large, some of them may cause appreciable errors. Accordingly, no attempt was made to refine and reduce either the data or the analysis. Some of the problems will be studied or avoided in future tests. The method of approach used to predict the force is consistent and comparatively simple.

CONCLUSION

Unsteadiness of flow can have a profound effect on resistance. Systematic measurements of the variation of force with time have formed the basis for a quantitative interpretation of the force exerted on a body in a time-dependent motion of a fluid. For flow past a flat plate, the manner in which the wake forms is vital in determining the resistance.

For the nearly simple harmonic motion at a node of a standing wave, the coefficient of virtual mass for the flat plate was found to vary from 1.1 to 1.8, approximately, the coefficient increasing with the size of the wake. Simultaneously, the coefficient of drag varied from about 5 to 3. The two coefficients are inversely related in a way which has been illustrated by an extension of Riabouchinsky's analysis. Although much remains to be studied, a means of satisfactorily describing the occurrence has been formulated.

APPENDIX

The calculation of the force variation with time was accomplished by first assuming a function $k(t)$. The drag coefficient $C_D(t)$ was then determined from Fig. 2. The velocity variation was assumed to be sinusoidal with time, and the quantity $k \sin \omega t$ was plotted. From this curve $d(kV)/dt$ was obtained graphically. These values were then substituted in Equation 1 and the force was calculated.

Early in the work the form of $k(t)$ was not known, except that it was apparent that k should be periodic and not have values less than 1. Analysis of the data indicated that at 90° (the moment of zero velocity) k would be 1.66 because the only contribution to the force is from the $k \, dV/dt$ term. However, no force curve could be obtained that came sufficiently close to the experimental values at other points (curve B in Fig. 9) for which 1.66 was used

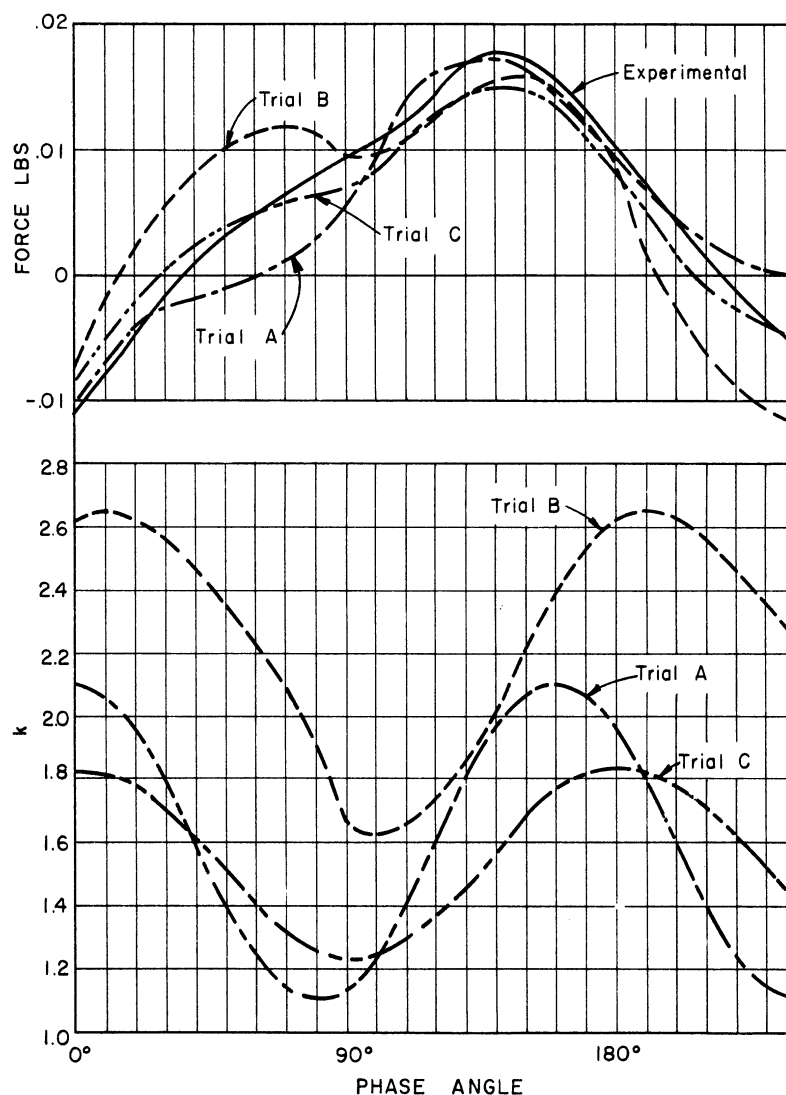


Fig. 9. Effect of $k(t)$ on force prediction.

as the minimum value of k . Hence, the requirement of an exact fit at 90° was abandoned in favor of a closer fit throughout the cycle. Other trials were made including sinusoidal variations of $k(t)$ (curve A in Fig. 9) until one leading to an acceptable correspondence was obtained (curve C in Fig. 9). Even for the rather similar variations assumed for the three cases shown, large differences are evident in various curves for $F(t)$. Accordingly, the empirical test restricts greatly the range of variability of k as defined in the simplified analysis leading to Equation 1.

REFERENCES

1. Lamb, H. Hydrodynamics. 6th ed. New York: Dover Publ., Inc., 1945.
2. Keulegan, G. H. Chapter XI, Engineering Hydraulics. Edited by H. Rouse. New York: John Wiley and Sons, Inc., 1950.
3. Riabouchinsky, D., "Sur la résistance des fluides," Comptes Rendus Congrès International des Mathématiciens, Strasbourg, 1920.
4. Birkhoff, G., Plesset, M., and Simmons, N., "Wall Effects in Cavity Flow - II," Quart. Appl. Math., 9 (Jan., 1952).
5. McNown, J. S. "Note on estimation of virtual mass coefficient." (Apr. 17, 1955, unpublished, Sandia Corp.)
6. Gilbarg, D., and Rock, D. H. Naval Ordnance Laboratory Memorandum 8718, 1945.
7. Roshko, A. A New Hodograph for Free-Streamline Theory. NACA TN-3168, 1954.
8. Westergard, H. M., "Water Pressures on Dams During Earthquakes," Trans. ASCE (1933).
9. McNown, J. S., "Hydrodynamic Earthquake Forces on Submerged Structures," Proceedings of the Third Midwestern Conference on Fluid Mechanics (1953).
10. Stelson, J. M., and Mavis, F. T., "Virtual Mass and Acceleration in Fluids," Proc. ASCE, Separate No. 670 (1955).
11. Yu, Yee-Tak, "Virtual Masses of Rectangular Plates and Parallelepipeds in Water," J. Appl. Physics (Nov., 1945); "Virtual Masses and Moments of Inertia of Disks and Cylinders in Various Liquids," ibid. (1942).
12. Caldwell, J. M. and Silberman, E., Discussion of the paper by Stelson and Mavis (Ref. 10), Proc. ASCE (Sept., 1955); Stelson, T. E., and Mavis, F. T., Discussion J. of the Engineering Mechanics Div., Proc. ASCE (Apr., 1956).
13. Reid, R. O., and Bretschneider, C. L., "The Design Wave in Deep Water or Shallow Water, Storm Tide, and Forces on Vertical Piling and Large Submerged Objects," A. and M. College of Texas, Dept. of Oceanography, Tech. Report on Contract N0y-27474, DA-49-005-eng-18, and N7onr-48704, 36 pp., Feb., 1954, unpublished.

REFERENCES
(concluded)

14. Iverson, H. W., and Balent, R., "A Correlating Modulus For Fluid Resistance in Accelerated Motion," J. Appl. Physics, 22 (Mar., 1951).
15. Keulegan, G. H., and Patterson, G. W., "Mathematical Theory of Irrotational Translation Waves," J. Res. Natl. Bur. Std. (Jan., 1940).

